Journal of Materials Chemistry C

Proton Damage Effects in Double Polymorph γ/β-Ga2O3 Diodes

Journal:	*Journal of Materials Chemistry C*
Manuscript ID	TC-ART-11-2023-004171.R1
Article Type:	Paper
Date Submitted by the Author:	11-Dec-2023
Complete List of Authors:	Polyakov, Alexander; Chonbuk National University, Vasilev, A.; National University of Science and Technology MISIS, Kochkova, Anastasia; National University of Science and Technology MISiS Schemerov, Ivan; National university of science and technology "MISiS", Department of new materials and nanotechnologies Yakimov, Evgeniy; Institute of Microelectronics Technology and High-Purity Materials Miakonkikh , Andrew; Valiev Institute of Physics and Technology of RAS Chernykh, A.; National University of Science and Technology MISIS, Lagov, Peter; National University of Science and Technology "MISiS," , The Laboratory of Advanced Solar Energy Pavlov, Yuri; Frumkin Institute of Physical Chemistry and Electrochemistry RAS, Laboratory of radiation technologies Doroshkevich, A.; Joint Institute for Nuclear Research, Isaev, R; Joint Institute for Nuclear Research Romanov, Andrey; National University of Science and Technology MISIS, Alexanyan, L; National University of Science and Technology "MISiS," , The Laboratory of Advanced Solar Energy Matros, N; National University of Science and Technology MISiS Azarov, Alexander; Oslo University, Department of Physics Kuznetsov, Andrej; Oslo University, Department of Physics Pearton, Stephen; Univ.Florida, MSE

ARTICLE

Proton Damage Effects in Double Polymorph γ/β-Ga_2O_3 Diodes

Alexander Y. Polyakov[a], Anton A. Vasilev[a], Anastasiia I. Kochkova[a], Ivan V. Shchemerov[a], Eugene B. Yakimov[a,b], Andrej V. Miakonkikh[c], Alexei V. Chernykh[a], Petr B. Lagov[a,d], Yrii S. Pavlov[d], A. S. Doroshkevich[e], R.Sh. Isaev[e], Andrei A. Romanov[a], Luiza A. Alexanyan[a], Nikolai Matros[a], Alexander Azarov[f], Andrej Kuznetsov[f**] and Stephen Pearton[g*]

Received 00th January 20xx,
Accepted 00th January 20xx

DOI: 10.1039/x0xx00000x

Double polymorph γ/β-Ga_2O_3 structures remain crystalline upon unprecedentedly high crystal disorder levels where other semiconductors lose their long-range symmetry and, eventually, become amorphous. However, it is unclear if this radiation tolerance translates to device-like operation, where much lower levels of damage degrade the performance. In this work, we fabricated conducting double polymorph γ/β-Ga_2O_3 structures using ion implantation and subsequent hydrogenation of the top γ-Ga_2O_3 layer, instead of conventional impurity doping which is limited by γ-Ga_2O_3 stability tradeoffs. While not a direct comparison, these structures exhibited much higher radiation tolerance compared to conventional Schottky diodes made of β-Ga_2O_3. Specifically, using 1.1 MeV proton irradiation at fluences of 10^{14}-10^{15} cm^{-2}, conventional β-Ga_2O_3 diodes became unfunctional, while double polymorph γ/β-Ga_2O_3 diodes remained operational. The centers supplying electrons in γ-Ga_2O_3 were characterized by prominent DX-like persistent photocapacitance. For samples implanted with Ga^+ and Si^+ to produce the $\beta \rightarrow \gamma$ transition, annealed at 600 °C and plasma hydrogenated, the net donor concentration was ~10^{12} cm^{-3}, with dominant electron traps near E_C-0.65-0.7 eV and photocapacitance and photocurrent spectra determined by deep acceptors with optical ionization thresholds 1.3 eV, 2 eV, 2.3 eV and 2.8 eV. Irradiation with 1 MeV protons increased the net donor density of these conducting γ/β-Ga_2O_3 structures, with carrier creation rates of (1.5-4.4)×10^{-2} cm^{-2}, in sharp contrast to the carrier removal rates of 150-200 cm^{-1} under identical conditions in the original β-Ga_2O_3 films.

Introduction

Ga_2O_3 is an ultra-wide bandgap semiconductor attracting attention because of its promising applications in power electronics and deep-UV photonics.[1–3] Up to date, most studies have focused on its thermodynamically stable monoclinic polymorph, β-Ga_2O_3. There is increasing interest in studies of the metastable polymorphs, specifically, corundum α-Ga_2O_3, orthorhombic κ-Ga_2O_3, and cubic γ-Ga_2O_3 phases.[4–11] Recently, it was found that double polymorph γ/β-Ga_2O_3 structures can be fabricated via disorder induced ordering in ion-irradiated β-Ga_2O_3, upon reaching a certain disorder threshold, resulting in a continuous γ-Ga_2O_3 film on top of the β-Ga_2O_3 substrate.[12–14] Such structures exhibit remarkably high radiation tolerance upon further ion irradiation.[15] Specifically, it was demonstrated that the top γ-Ga_2O_3 film remains crystalline for unprecedentedly high disorder levels, at which all other known semiconductors lose their long-range symmetry and, eventually, become amorphous.[15] Thus, double polymorph γ/β-Ga_2O_3 structures constitute a new class of materials of intertest for electronics, if in addition to their ability to withstand the amorphization, the devices made of these materials demonstrate the radiation tolerance in terms of the electronic properties.

The double polymorph γ/β-Ga_2O_3 structures formed via irradiation exhibit rather high electrical resistivity in their "as-fabricated" state. Indeed, the reason for γ-Ga_2O_3 to be capable to maintain its crystalline lattice under irradiation was explained by a high density of native defects leading to "self-healing" of the radiation-induced defects assisted by the interactions with native defects.[15] In conventional semiconductors, defect-related electrical compensation upon irradiation is usually removed by anneals and/or extrinsic doping followed by anneals. However, applying similar strategy for the double polymorph γ/β-Ga_2O_3 structures is difficult because of their limited thermal stability. Indeed, γ-Ga_2O_3 is naturally metastable, converting to β-Ga_2O_3 upon anneals, so that anneals at temperatures above 600 °C are sufficient for igniting this process.[16] In this context, recent attempts to activate ion-implanted Si donors by such relatively low temperature anneals in γ-Ga_2O_3 (≤ 600 °C), have not resulted in achieving sufficient conductivity control,[17] consistent with the fact that much higher temperatures (>900°C) were reported to activate ion implanted Si donors in β-Ga_2O_3.[18]

[a] National University of Science and Technology MISIS, Moscow, Leninsky pr. 4, Moscow 119049, Russia
[b] Institute of Microelectronics Technology and High Purity Materials, Russian Academy of Sciences, 6 Academician Ossipyan str., Chernogolovka, Moscow Region 142432, Russia
[c] Valiev Institute of Physics and Technology, Russian Academy of Sciences, Moscow, 117218, Nahimovsky Ave, 36(1), Russia
[d] Laboratory of Radiation Technologies, A. N. Frumkin Institute of Physical Chemistry and Electrochemistry Russian Academy of Sciences, Moscow 119071, Russia
[e] Joint Institute for Nuclear Research, Joliot-Curie 6, Dubna, Moscow Region, 141980, Russia
[f] Department of Physics, Centre for Materials Science and Nanotechnology, University of Oslo, N-0316 Oslo, Norway
[g] Department of Materials Science and Engineering, University of Florida, Gainesville, FL 32611, USA

Electronic Supplementary Information (ESI) available: [details of any supplementary information available should be included here]. See DOI: 10.1039/x0xx00000x

However, simultaneously, it was shown that hydrogenation of the γ-Ga_2O_3 film on the top of the β-Ga_2O_3 may be used as a method to achieve the n-type conductivity.[17] Indeed, hydrogen and/or hydrogen-related complexes are known to act as electrically active defects in semiconductors and frequently as donors in oxides.[19]

The increase of the net donor concentration after the H plasma treatment has been shown recently to be a common feature of all polytypes of Ga_2O_3 under certain treatment conditions and can be attributed to the processes common for all of them and possibly ascribable to the formation of Ga vacancy complexes with 4 H atoms.[20] The effect of Ga_2O_3 interactions with various plasmas is in general an interesting and fruitful area of research in which intriguing and potentially useful phenomena, such as a giant increasing of the photosensitivity of Schottky diodes after the treatment in Ar plasma[21] or a marked increase of the N solubility and the formation of GaNO after the treatment in N plasma[22] have been recently reported.

Thus, the prime aim of this work was to demonstrate that the β-Ga_2O_3 samples converted to γ-Ga_2O_3 at the surface by implantation of Ga or Ga and Si and subsequent H plasma treatment can be processed into useful Schottky diodes with reasonably good leakage current, rectification, photosensitivity in the UV spectral region, to subject these samples to high energy particles irradiation, and to compare the changes induced in electrical properties by such irradiation with those occurring in more established semiconductor materials in order to check whether the high radiation tolerance of γ/β-Ga_2O_3 structures in terms of the lack of amorphization will also be accompanied by the slower changes of electrical and photoelectrical properties. As a benchmark against which such comparison is done we have chosen Schottky diodes prepared on commercial β-Ga_2O_3 structures. And the high energy particles irradiation with 1.1 MeV protons was selected as a representative irradiation source. The radiation effects in β-Ga_2O_3 have been extensively studied and have been reviewed in several papers.[9,23,24] The main bulk of these studies relates to the high energy particles predominant in the radiation belts surrounding Earth and consisting of electrons of energies in some MeV range and protons in the same energy range, with some work also done for fast neutron irradiation, alpha-particles irradiation, γ-irradiation.[9,23,24] Such data are of most importance for low-orbit space military and commercial applications and for ground military and civil applications.[9,23,24] In these categories of high energy particles it has been demonstrated that the radiation tolerance of β-Ga_2O_3-based devices is among the highest.[9,23,24] Of course, for open space applications, much higher energies of particles and a much higher range of particles of interest is of interest. Such studies are being carried out for different semiconductors, the radiation tolerance of β-Ga_2O_3 devices to protons in the 100 MeV – 1 GeV range,[25,26] and to irradiation with high energy heavy ions have been published[27–29] and also demonstrate a high radiation tolerance of β-Ga_2O_3 devices. Thus, comparing the radiation tolerance of γ/β-Ga_2O_3 test devices to that of β-Ga_2O_3 devices looks as a justified measure of the radiation-tolerance worthiness of the γ/β-Ga_2O_3 samples in electronic sense. We have chosen for such comparisons the proton energy of 1.1 MeV for the proton fluences range of 10^{14}-10^{15} p/cm^2 as this is a well characterized proton energy range for which the measurable changes in the properties of β-Ga_2O_3 can be easily detected.[17,30] These comparative studies have enabled us, for the first time, to demonstrate that the radiation tolerance of the γ/β-Ga_2O_3 samples is not only very high in terms of crystalline quality, but also high in terms of electronic properties. We also present for the first time the deep trap spectroscopic data for γ-Ga_2O_3, as affected by proton irradiation.

Experimental

Double polymorph γ/β-Ga_2O_3 structures were fabricated by ion implantation into (010)-oriented Fe doped semi-insulating β-Ga_2O_3 single crystals purchased from Tamura Corporation. Two types of implants were used: either room temperature single 1.7 MeV Ga^+ implants with a fluence of 6×10^{15} Ga/cm^2 or the same Ga implants followed by an elevated temperature box-profile Si implants using energies (and fluences) of 300 keV (10^{15} Si/cm^2) and 36 keV (2×10^{14} Si/cm^2). The rationale behind these combinations was to fabricate γ-Ga_2O_3 on the top of the β-Ga_2O_3 substrate by the Ga implants,[13,14] and try to activate Si donors via elevated temperature implants.[31] For clarity, the samples were labelled as γ-GaO1 for implantation with only Ga^+ and γ-GaO2 and γ-GaO3 for those additionally implanted with Si^+ ions at 200 °C and 400 °C, respectively. Notably, sample γ-GaO2 was also subjected to 600 °C post-irradiation rapid thermal annealing. Further, because Si donor activation was low, all these samples were subjected to a hydrogen plasma treatment for 0.5 h at 330 °C.[17,18] Structural characterizations of implanted, annealed and H plasma treated identical samples were reported previously.[15,17] These measurements confirmed that the selected sample fabrication conditions result in the double polymorph γ/β-Ga_2O_3 structures with the top γ-Ga_2O_3 layer thickness of ~950 nm in the as-fabricated state, slightly decreasing upon anneals.[15,17]

A brief summary of structural characterization of these samples as reported in detail[13,15,17] and confirming the formation of heterojunction of γ/β-Ga_2O_3 with sharp interface and the changes of electronic properties after implantation and annealing is presented for the readers benefit in the Supplementary Material together with the Fig. S1 of the Supplementary Material. For comparison, we used Sn-doped (010)-oriented β-Ga_2O_3 single crystals purchased from Tamura Corporation, labeled as β-GaO1 and β-GaO2, and having net donor density of 4.6×10^{16} cm^{-3} and 3.8×10^{17} cm^{-3}, respectively.

Electrical characterization, including deep trap spectra, photocurrent and photocapacitance spectra, were performed on Schottky diodes fabricated on all the samples described above, having semi-transparent Ni rectifying and Ti/Au Ohmic contacts, both deposited on the top surface of the samples subjected to implantation and H plasma treatments. The measurements were performed in dark and under monochromatic illumination of Light Emitting Diodes (LEDs), with peak wavelengths between 950 nm and 277 nm.[32]

We performed such dark/illumination combinations for capacitance versus frequency (C-f), capacitance-voltage (C-V),

current-voltage (I-V) and current versus temperature (I-T) measurements. Further, we performed Thermally Stimulated Current (TSC), Admittance Spectroscopy (AS), Current Deep Level Transient Spectroscopy (CDLTS), Photoinduced Current Transient Spectroscopy (PICTS), as well as Deep Level Transient Spectroscopy with electric (DLTS) and optical (ODLTS) injection. All these measurements were performed on the as-fabricated diodes, followed up by repeating the measurements after 1.1 MeV protons irradiations with fluences of 2×10^{14} p/cm^2 and 2×10^{15} p/cm^2 for *γ*-GaO2 and *γ*-GaO3 samples, respectively.

The necessity of using a variety of electrical characterization techniques above is dictated by the fact that the samples are not well suited for straightforward DLTS/ODLTS characterization because of the rather high series resistance of the samples, and the energy depth and concentration of deep electron and hole traps compared to the density of shallow donors. And this is particularly true for analysis of the properties of the *β*-Ga_2O_3 samples after proton irradiation. This required doing preliminary TSC and low-frequency AS measurements to determine the position of the major traps pinning the Fermi level that could change their occupation upon illumination. DLTS measurements of the spectra of deep electron traps in the upper ~E_C-1.2 eV portion of the bandgap in DLTS and of hole traps with depths ~E_V+1.2 eV from the valence band edge in ODLTS using the custom designed DLTS system capable of operation at low frequencies starting from 1 kHz, thus alleviating problems with high series resistance, was necessary.[33] One also has to perform C-V measurements under monochromatic illumination to detect

and characterize very deep donors and acceptors throughout the width of the bandgap, and to complement DLTS/ODLTS measurements with their current CDLTS/PICTS counterparts. [32,34–36]

For comparison, diodes fabricated on the *β*-GaO1 and *β*-GaO2 samples were also irradiated with 1.1 MeV protons, with fluences 2×10^{14} p/cm^2 and 2×10^{15} p/cm^2, respectively. Table 1 summarizes all studied samples, treatments, and resulting carrier densities. For extraction of carrier traps parameters from the data measured in *γ*-Ga_2O_3, the effective mass of electrons was assumed to be the same as in *β*-Ga_2O_3. Importantly, *γ*-GaO1 was not subjected to the irradiation tests because of its too high carrier concentration and, consequently, lower reliability of the Schottky diodes. Detailed descriptions of the electrical measurements setups and proton irradiation setup can be found elsewhere.[33–37]

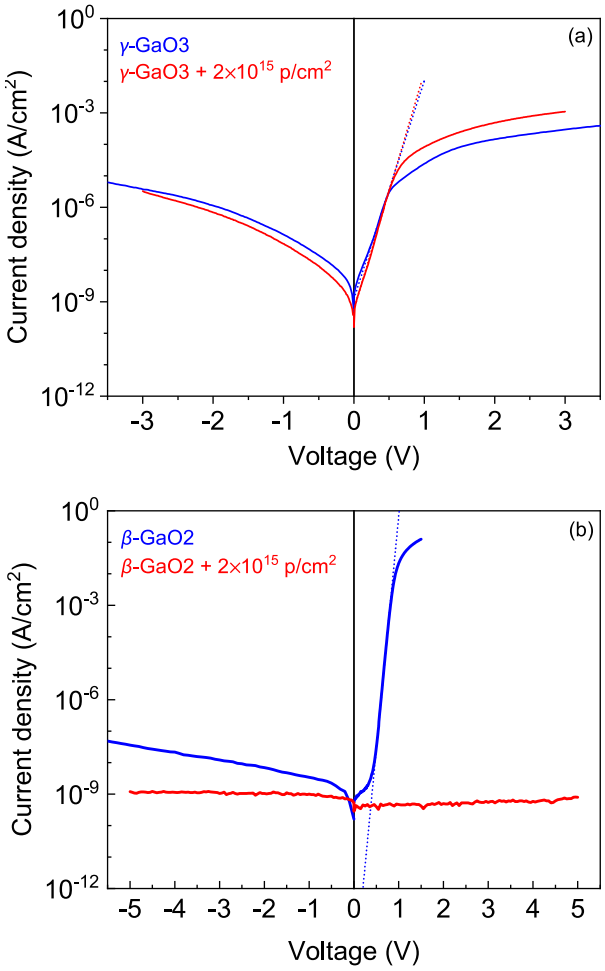

Fig. 1 Comparison of I-V characteristics of (a) *γ*- and (b) *β*-Ga_2O_3 Schottky structures demonstrating 2×10^{15} p/cm^2 1.1 MeV protons tolerance of *γ*-GaO3 sample.

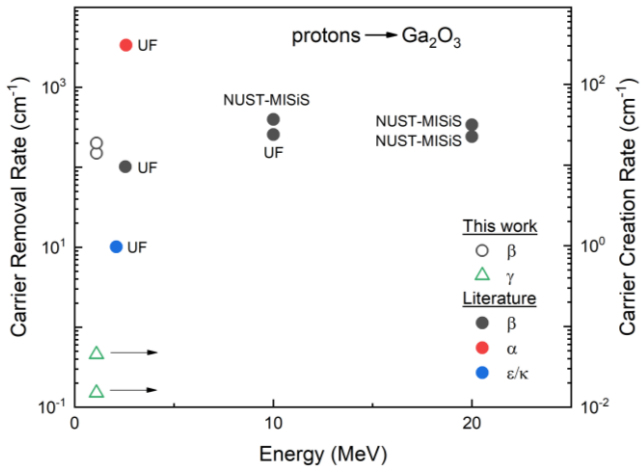

Fig. 2 Carrier removal and creations rates of Ga_2O_3 polymorphs for different protons energies.

Results

Firstly, in "as-fabricated" states, all double polymorph γ/β-Ga_2O_3 structures, independently whether they were produced via single Ga or dual Ga + Si implants, exhibited high electrical resistivity. Consistent with literature data,[17,18] it confirmed that even elevated temperature Si ion implants followed by anneals at temperatures not exceeding γ-Ga_2O_3 stability limits were insufficient for efficient donor activation in γ-Ga_2O_3. Secondly, the hydrogenation affected samples γ-GaO1 and γ-GaO2 or γ-GaO3 in two different ways. Specifically, Fig. S2 in the Supplementary Material summarizes electrical characterization of γ-GaO1 upon hydrogenation. Fig. S2(b) depicts the carrier concentration profile, reaching 10^{19} cm^{-3} range in the vicinity of the surface. Thus, this diode was not used in further irradiation tests, even though some interesting capacitance data were collected from γ-GaO1 as summarized in Fig. S2. Accordingly, in the rest of the paper we will mainly discuss the behavior of γ-GaO2 and γ-GaO3 samples since, upon the hydrogenation, they exhibited carrier concentrations enabling the radiation tests and spectroscopic studies.

While not a direct comparison of radiation stability, Fig. 1 shows the minimal effect of proton irradiation at a fluence of 2×10^{15} p/cm^2 on the I-V characteristics of the double polymorph γ/β-Ga_2O_3 diodes. By sharp contrast, the same fluence renders the β-Ga_2O_3 diodes insulating down to the depth corresponding to the range of 1.1 MeV protons in β-Ga_2O_3. Table I summarizes the net donor concentration changes in the two studied β-Ga_2O_3 samples with different starting donor concentrations of 4.6×10^{16} cm^{-3} (β-GaO1) and 3.8×10^{17} cm^{-3} (β-GaO2) (respective starting $1/C^2$ versus V plots are presented in Fig. S3(a) of the Supplementary Material, the starting C-f characteristics are shown in Fig. S3(b) of the Supplementary Material. Irradiation of the more lightly doped γ-GaO1 sample with 2×10^{14} p/cm^2 fluence of 1.1 MeV protons led to the upper ~9 μm portion of the sample being totally depleted of electrons which was manifested in the strong decrease of capacitance in Fig. S3(b), with the capacitance corresponding to the "geometric" capacitance of the 8.6 μm-thick dielectric β-Ga_2O_3 layer. Thus, all the starting shallow donors in the top portion of the film have been compensated giving the effective carrier removal rate of 230 cm^{-1}. For the more heavily doped sample β-GaO2 the irradiation with the fluence of 2×10^{14} p/cm^2 1.1 MeV protons resulted in the decrease of the net donor density to 3.4×10^{17} cm^{-3}, corresponding to the carrier removal rate of 200 cm^{-1}. Further irradiation of this sample to 2×10^{15} p/cm^2 fluence completely compensated all shallow donors in the top ~9 μm-thick layer, resulting in the capacitance of the structure becoming as low as for the irradiated sample β-GaO1 (Fig. S3(b)

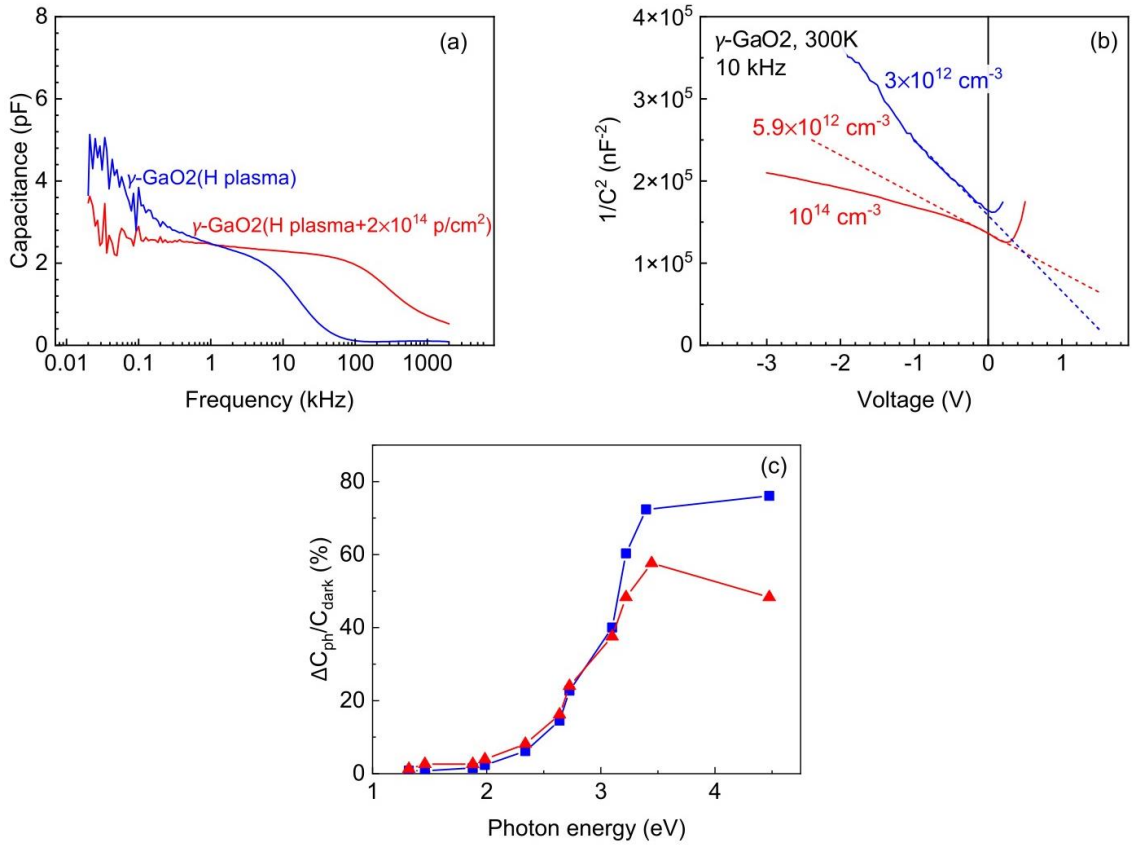

Fig. 3 (a) Room temperature C-f dependencies measured for sample γ-GO2 after H plasma treatment (blue line) and after additional irradiation with 2×10^{14} p/cm^2 1.1 MeV protons (red line); (b) room temperature C-V characteristics measured at 10 kHz after H plasma treatment (blue line) and after irradiation with 2×10^{14} p/cm^2 protons (red line) (the numbers near the curves indicate the calculated concentrations); (c) photocapacitance spectra measured after H plasma treatment (blue line) and after additional irradiation with 2×10^{14} p/cm^2 protons.

of the Supplementary Material). The width of the β-Ga_2O_3 region fully depleted of electrons is in close agreement with the estimated range of 1.1 MeV protons in β-Ga_2O_3 (Fig. S4(a) of the Supplementary Material). This happens for even a quite moderate number of diplacements per atom (Fig. S4(b)) and results in the samples completely loosing rectification because of the very high resistance of the irradiated region., as shown in Fig. 1. The photosensitivity of the Schottky diodes also decreased dramatically because of the very high series resistance of the damaged layer. The spectra of deep traps in this layer could be measured by PICTS and showed the presence of high densities of deep traps with energy levels at E_c-0.65 eV, E_c-0.82 eV, and E_c-1.2 eV (Fig. S5 of the Supplementary Material). The observed carrier removal rates and the types of defects predominant in irradiated β-Ga_2O_3 are in general agreement with published data.[9,30] The story is totally different for the γ/β-Ga_2O_3 polymorph structures where the carriers were actually created at a low rate of 0.025-0.04 cm^{-1} (see below). Fig. 2 summarizes the reported carrier removal rates from the literature during proton irradiation at different energies in the different polymorphs of Ga_2O_3. Current results obtained for the γ/β-Ga_2O_3 samples studied in this paper are also shown. Note that in the other three polymorphs, carriers are removed by creation of trap states, at rates that depend somewhat on the polymorph, with the ε/κ polymorph having lower rates than β- or α-Ga_2O_3. Remarkably, the γ-polymorph does not lose carriers at all during high fluence proton irradiation, but rather picks them up at a low rate. The actual physical nature of the process needs yet to be understood.

Fig. 3 summarizes the results of the C-f and C-V measurements of the γ-GaO2 diodes before and after proton irradiation (the actual C-f spectra measured in the dark and under monochromatic illumination are presented in Fig. S6(a, b) of the Supplementary Material). Before the H plasma treatment the sample showed no measurable capacitance because of the very high resistance of the layer.[17] After the H plasma treatment, as shown in Fig. 3(a), there appeared a measurable capacitance at low frequencies. C-V measurements performed at frequencies corresponding to the plateau in the C-f dependence on Fig. 3(a), when plotted in the usual $1/C^2$ versus V form, yielded the net shallow donors concentration of 3×10^{12} cm^{-3} at 300 K. The proton irradiation changed the carrier density slightly increasing it to 5.2×10^{12} cm^{-3} near the surface and to 10^{14} cm^{-3} deeper inside the sample (see red-color lines in Fig. 3(b)). However, the γ-GaO2 diode remained fully operational in contrast to the β-GaO1 diodes exposed to the same irradiation that became non-functional due to electrical compensation, (see Fig. S3 of the Supplementary Material). In general, γ-GaO2 diodes showed good rectification (see Fig. S7 of the Supplementary Material) as well as measurable photocapacitance (Fig. 3(c)) and photocurrent (Fig. 4, the actual I-V characteristics measured in the dark and under monochromatic illumination are shown in Fig. S7(a, b) of the Supplementary Material), proving that γ-Ga_2O_3 thus prepared has potential for device applications Furthermore, Fig. 3(c) that illustrates the changes in the spectral dependence of the photocapacitance ΔC_{ph} normalized by the dark capacitance C_{dark} as measured at 10 kHz (the blue line) before and after proton irradiation proves that photocapacitance changes with irradiation are quite low. Overall, the photocapacitance spectra were not radically changed by the proton irradiation, displaying optical ionization thresholds at 1.3 eV, 2 eV, 2.8 eV, and 3.1 eV. Interestingly, the spectral dependence of photocapacitance is not all that different from the spectral dependence in β-Ga_2O_3.[9,32,34,36] Mind also that the peak photocurrent value at -3V after irradiation decreased only by about 2 times (Fig. 4).

The series resistance of the diodes is high explaining the photosensitivity in both bias directions. This is also manifested in the C-f characteristics under illumination, with the roll-off frequency determined by the series resistance increasing with illumination (see Fig. S3 of the Supplementary Material).

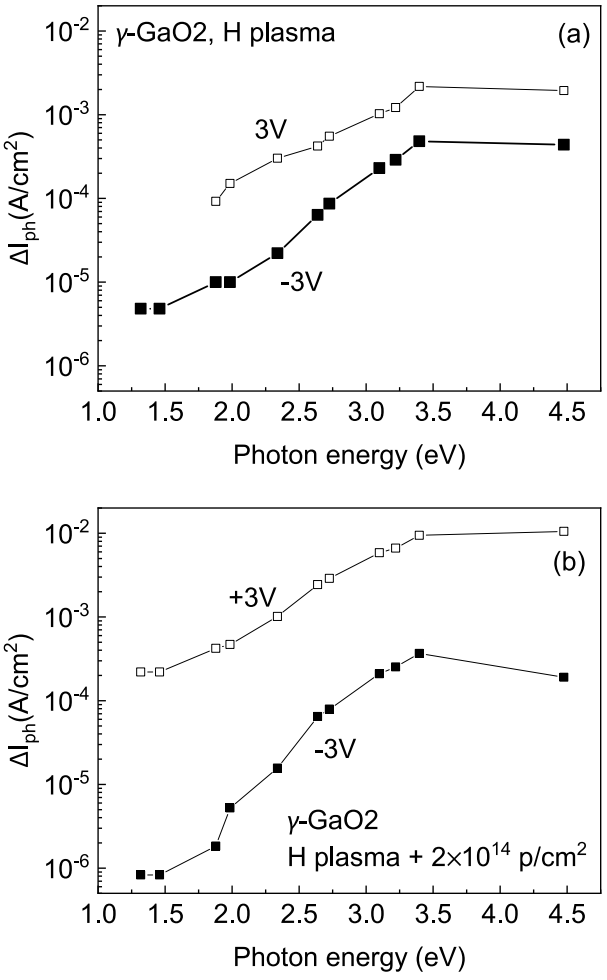

Fig. 4 Spectral dependencies of photocurrent at -3V and 3V for γ-GaO2 sample after H plasma treatment; (b) the same for additional irradiation with 2×10^{14} p/cm^2 1.1 MeV protons.

The spectra of deep traps in this sample before proton irradiation was characterized by the predominance of electron traps with levels near E_c-0.7 eV and electron capture cross section $\sigma_n=1.3\times10^{-16}$ cm^2. Fig. 5 presents the CDLTS spectra (the temperature dependence of CDLTS signal $\Delta I=I(t_2)-I(t_1)$ normalized by the steady state current, $\Delta I/I$) taken with the bias on the sample of -2V and forward bias pulse of 1V applied for

1 s (t_1 and t_2 here are as usual the time windows, their values are specified in the figure caption). These traps were also detected in DLTS spectra measured at the low probing frequency of 10 kHz, and in high temperature admittance spectra (the actual spectra not shown here). Upon the proton irradiation the peak corresponding to the E_C-0.7 eV trap has vanished and instead a weaker peak corresponding to a trap with level near E_C-1 eV has emerged, thus indicating a serious transformation of defect states due to interaction with radiation defects.

The *γ*-GaO3 diodes behaved qualitatively similar to *γ*-GaO2 diodes in terms of the electrical performance and radiation tolerance, as shown in Figs.6-8. For example, room temperature capacitance versus frequency dependences in Fig. 6(a) showed the existence of measurable capacitance for frequencies up to 100 kHz after the H plasma treatment of the sample. The net donor concentration determined from the $1/C^2$ versus voltage plot in Fig. 6(b) gave the value of 3.5×10^{12} cm^{-3} before irradiation. After proton irradiation with the fluence of 2×10^{15} p/cm2 the net donor concentration again increased (to 8.7×10^{13} cm^{-3}) as for sample *γ*-GaO2, confirming that protons were not compensating donor conductivity, but rather supplying additional donors. (Admittance spectra measured after irradiation showed that the donors in question had the ionization energy of 0.3 eV (Fig. S8(a,b) of the Supplementary Material). Similarly, the photocapacitance measurements data were qualitatively the same for *γ*-GaO2 and *γ*-GaO3, as illustrated by comparison of Figs. 3(c) and 6 (c). As in Fig. 3(c), the optical ionization thresholds in sample *γ*-GaO3 before irradiation are close to 1.3 eV, 2.3 eV, and 3.1 eV.

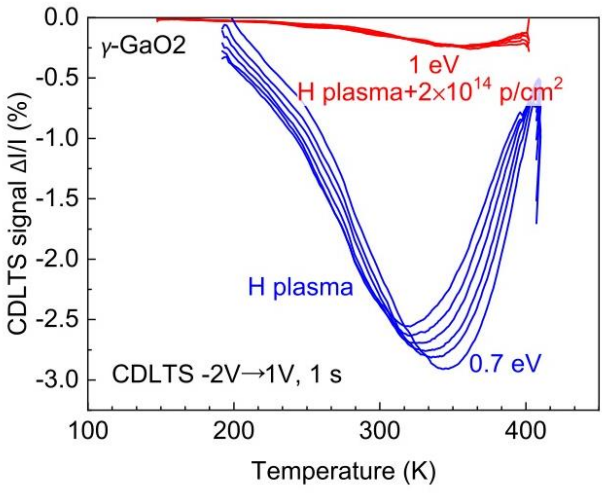

Fig. 5 CDLTS spectra ΔI/I measured at the bias of -2V and forward bias pulse 1V (1 s long) for sample *γ*-GaO2 after H plasma treatment, the relaxation curves are presented for time windows of 150 ms/750 ms, 300 ms/1500 ms, 450 ms/2250 ms, 750 ms/3750 ms, 1200 ms/6000 ms (blue lines); the red spectra were obtained after additional irradiation with 2×10^{14} p/cm^2 1.1 MeV protons.

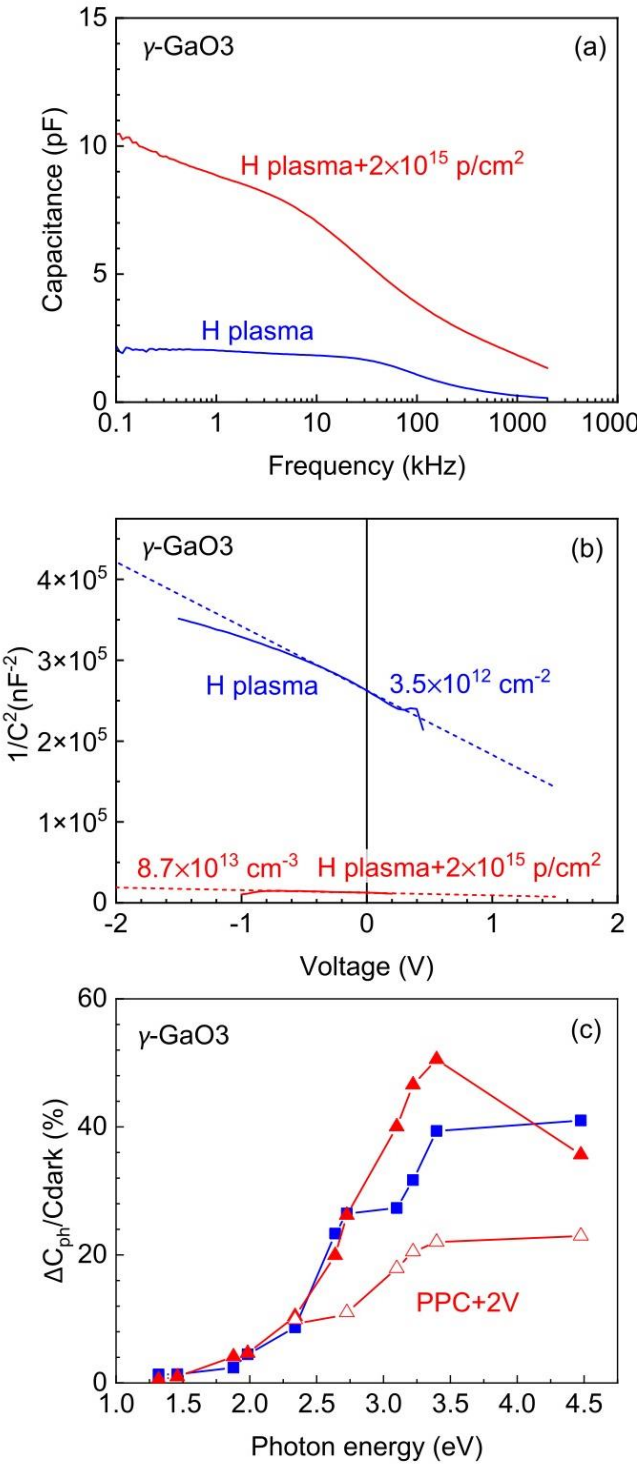

Fig. 6 Room temperature (a) C-f, (b) C-V and (c) LCV characteristics for sample *γ*-GaO3 after treatment in H plasma and after additional irradiation with 2×10^{15} p/cm2 1.1 MeV protons.

Measurements of capacitance after switching the light off showed that considerable part of photocapacitance was persistent and could not be quenched even by application of the forward bias of 2V (see the curve formed by open triangles for the sample after irradiation in Fig. 6(c) labeled as "PPC+2V") suggesting that respective centers have a barrier for capture of

electrons.[9,32] Similar centers are observed in other Ga_2O_3 polymorphs.[9,30,34–36] The optical threshold for these persistent transitions is around 2 eV. After 2.3 eV the contribution of persistent capacitance centers becomes less pronounced. Irradiation enhances the cof such centers with optical threshold near 2.3 eV at the expense of the centers with optical threshold near 3.1 eV in samples before irradiation (compare the lines with blue squares and solid triangles in Fig. 6(c)). The nature of these changes needs to be better understood.

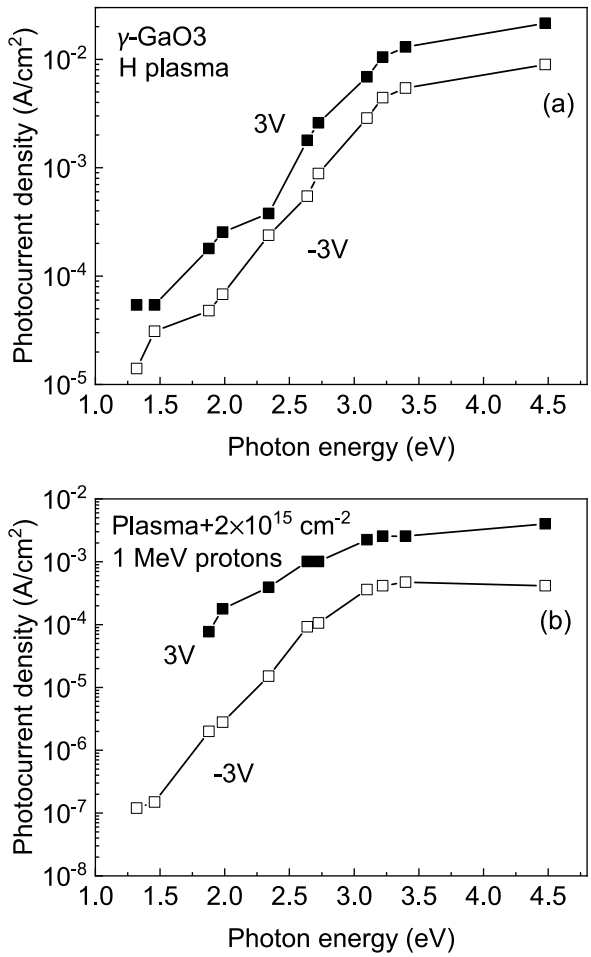

Fig. 7 (a) Photocurrent spectra for sample *γ*-GaO3 after H plasma treatment; (b) after additional irradiation with 2×10^{15} p/cm^2 1.1 MeV protons.

Photocurrent spectra before and after irradiation with the proton fluence of 2×10^{15} p/cm2 measured at -3V and +3V are compared in Fig. 7(a, b). As for the previous sample measurable photocurrent could be observed for both reverse and forward biases of -3V and 3V, the peak photocurrent values are substantially (about an order of magnitude) higher than for sample *γ*-GaO2, but the amount of photocurrent decrease induced by irradiation is also much higher which is understandable given an order of magnitude higher proton fluence.

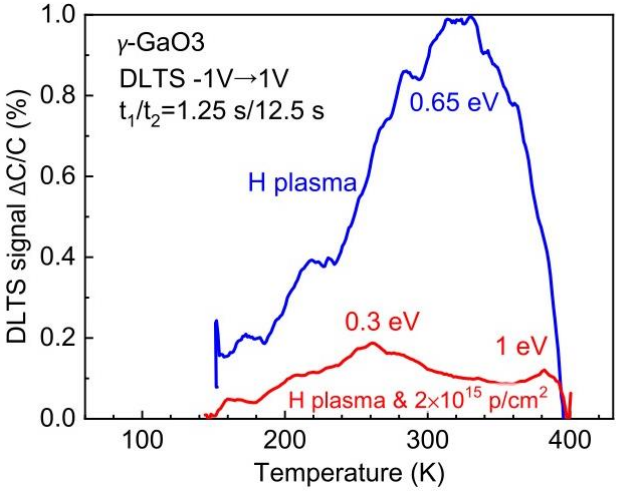

Fig. 8 DLTS spectra for sample *γ*-GaO3 after H plasma treatment (blue) and after additional irradiation with 2×10^{15} p/cm^2 1.1 MeV protons (red)

Fig. 8 shows the results of the DLTS measurements of the *γ*-GaO3 diodes using the low probing frequency of 10 kHz.[33] The data collected before proton irradiation reveal a trap at E_C-0.65 eV with electron capture cross section of $\sigma_n=5\times10^{-17}$ cm^2, consistent with the CDLTS data for *γ*-GaO2 in Fig. 5. Similar to what was observed for the *γ*-GaO2 diode, upon proton irradiation of *γ*-GaO3 diodes, we observe a strong suppression of the dominant E_C-0.65 eV trap in favor of the E_C-1 eV trap as well as an additional level at E_C-0.3 eV. The latter is the same center detected in AS spectra in Fig. S8(a, b) of the Supplementary Material.

Discussion

Our systematic analysis of electrical and photoelectrical properties of the double polymorph *γ*/*β*-Ga_2O_3 diodes in Figs. 3-8 confirms that these diodes exhibit reasonably good rectification, withstanding proton irradiation with very high doses, in contrast to what we observe in conventional *β*-Ga_2O_3 diodes. Importantly the proton fluence range of 10^{14}-10^{15} p/cm^2 investigated in this work is rather high and the radiation tolerance of the double polymorph *γ*/*β*-Ga_2O_3 diodes is indeed remarkable. For comparison, for Si and SiC diodes having similarly low carrier concentrations in the active diode region, degradation was already present for ~5×10^{11} and ~7×10^{12} cm^{-2} 1 MeV proton fluences, respectively.[34] The present demonstration of the radiation tolerance of *γ*/*β*-Ga_2O_3 samples paves the way for further detailed studies of double polymorph *γ*/*β*-Ga_2O_3 diodes, which are certainly necessary to shed the light on the mechanisms of the donor activation upon the hydrogenation in *γ*-Ga_2O_3 as well as to explain the evolution and interplay between shallow and deep levels upon the irradiation.

There are many open questions starting from the differences between the impact of hydrogenation on the *γ*-GaO1 samples compared to the *γ*-GaO2 and *γ*-GaO3 samples. These might be attributed to the effect of additional Si implants in samples *γ*-GaO2 and *γ*-GaO3. Assuming similarities in the

formation of hydrogen related complexes in *γ*- and *β*-Ga_2O_3, one may speculate on potential analogies for the impact of Si in these samples. For example, in *β*-Ga_2O_3, in our earlier work, we observed a deep donor formation at E_C-0.6 eV, so called E1 centers, as a result of the interaction of Si donors and H_i^- acceptors;[38] also theoretically predicted.[39] As such, the deep level dominating *γ*-Ga_2O_3 CDLTS and DLTS spectra before irradiation may be potentially attributed to Si-H complexes, because of its similar bandgap position and the availability of both Si and H. The nature of defects interaction causing the suppression of the E_C-0.65 eV trap and the emergence of the E_C-0.3 eV and E_C-1 eV levels is not clear at the moment and remains to be identified.

In contrast, in *γ*-GaO1 exhibiting much higher carrier concentrations, H obviously occurs in shallow donor configuration(s), also responsible for strong persistent photoconductivity and photocapacitance (see Fig.S1), indicating that the centers have a sizable barrier for capture of electrons, similar to so-called DX-like defects.[19] Notably, similar behavior was recently reported for hydrogenated *β*-Ga_2O_3 [40] and *κ*-Ga_2O_3 [41] films as well. In that context, it seems that H behaves similarly in Ga_2O_3 polymorphs even though the symmetry of the *β*-, *κ*-, and *γ*-polymorphs and consequently the energetics of the different H configurations are different. This may indicate that the centers of interest should involve simple defects to be found in all the polymorphs in which they've been detected.

Detailed theory of defect states has been developed for *β*-Ga_2O_3,[19,30,39,42] with some preliminary work also reported for *α*-Ga_2O_3.[43,44] In *β*-Ga_2O_3, possible candidates to be considered are isolated interstitial hydrogen donors H_i^+, hydrogen complexes with oxygen vacancies HO^+, and four- hydrogen ions complexes with Ga vacancies or split Ga vacancies $(V_{Ga}\text{-}4H)^+$ or $(V_{Ga}^i\text{-}4H)^+$.[30,39,42] The behavior of hydrogen interstitials H_i^+ or HO^+ complexes will probably not differ much between the different polymorphs, although, in *β*-Ga_2O_3 the complexes with oxygen vacancies yield shallow donors only for O vacancies in O1 and O3 positions, whereas, in O2 position the complex is expected to be a negative-U acceptor with the charge transition level near E_C-0.7 eV.[39] However, if judged by the results obtained for *β*-Ga_2O_3, all these defects are highly mobile and not very likely to be encountered in isolated form.[30,39] On the other hand, gallium vacancies (V_{Ga}) are expected to be stable, whether they occur in unrelaxed or split configurations,[30,39] and the formation of such complexes was used to explain a strong increase in shallow donor concentration in hydrogenated *β*-Ga_2O_3.[40,42] Thus, accepting V_{Ga} to be the dominant acceptor defects in other Ga_2O_3 polymorphs,[43] it is tempting to assume that the shallow defects supplying electrons in *γ*-GaO1 samples are related to V_{Ga} in either unrelaxed or split configurations forming complexes with 4 hydrogen interstitials.

Table 1 Samples studied , changes in concentration

Sample	Description	Treatments	n (cm^{-3})
γ-GaO1	EFG *β*-Ga_2O_3 (010), semi-insulating (Fe doped), Ga implanted at 300 K, 1.7 MeV, 6×10^{15} cm^{-2}	H plasma, 330°C	10^{19}
γ-GaO2	EFG *β*-Ga_2O_3 (010), semi-insulating (Fe doped) Ga implanted at 300 K, 1.7 MeV, 6×10^{15} cm^{-2} & Si implanted* at 200 °C and annealed to 600 °C	H plasma, 330°C	3×10^{12}
		1.1 MeV protons, 2×10^{14} p/cm^2	5.3×10^{12}
γ-GaO3	EFG *β*-Ga_2O_3 (010), semi-insulating (Fe doped), Ga implanted at 300 K, 1.7 MeV, 6×10^{15} cm^{-2} & Si implanted* at 400 °C	H plasma, 330°C	3.5×10^{12}
		1.1 MeV protons, 2×10^{15} p/cm^2	8.7×10^{13}
β-GaO1	EFG *β*-Ga_2O_3 (010), Sn doped	As-grown	4.3×10^{16}
		1.1 MeV protons, 2×10^{14} p/cm^2	High resistivity
β-GaO2	EFG *β*-Ga_2O_3 (010), Sn doped	As-grown	3.8×10^{17}
		1.1 MeV protons, 2×10^{14} p/cm^2	3.4×10^{17}
		1.1 MeV protons, 2×10^{15} p/cm^2	High resistivity

* Si implantation parameters are 300 keV with 10^{15} cm^{-2} + 36 keV with 2×10^{14} cm^{-2}

Conclusions

In this work, we fabricated double polymorph γ/β-Ga_2O_3 diodes using hydrogenation of the top γ-Ga_2O_3 layer formed by heavy ion implantation. The electronic properties of such structures as affected by proton implantation have been studied in some detail for the first time, which is of considerable fundamental interest, because the inferior crystalline properties of γ-Ga_2O_3 films obtained by growth at low temperatures makes such studies extremely unreliable. It has been shown that Schottky diodes fabricated on γ/β-Ga_2O_3 structures prepared by implantation and hydrogenation show reasonably good rectification and photosensitivity and thus possess some device potential. Although the attained performance is not exceptionally good some means of improving by changing the type and fluence of implanted species, the temperature of implantation, the regimes of hydrogenation seem to be open to optimization.

These studies could be of potential practical importance because the γ/β-Ga2O3 structures demonstrate a much higher proton radiation tolerance compared to conventional diodes made of β-Ga_2O_3. Specifically, upon 1.1 MeV proton irradiation with fluences in the range 10^{14}-10^{15} p/cm^2, for which conventional β-Ga_2O_3 diodes became unfunctional, the double polymorph γ/β-Ga_2O_3 based diodes remained operational. As the radiation tolerance of β-Ga_2O_3 devices has been shown to be exceptionally high, pursuing this area of research could hopefully pave the way to developing power devices and solar-blind photodetectors with truly outstanding radiation tolerance.

In contrast to other polymorphs of Ga_2O_3 in which radiation generally results in carrier removal due to compensation by radiation defects, in γ-Ga_2O_3 proton irradiation in fact leads to a slight increase in carrier density, which is an interesting and unusual physical phenomenon needing explanation. The removal rate is in a large part determined by the difference between the position of electrical neutrality level and the level of compensation defects. Hence the lower the electron concentration the lower in general will be the removal rate. For β-, α- and κ-material, the films have starting carrier concentrations in the range of interest for devices. With the γ-layers, the apparent concentrations are very low, so that quantitative comparisons of radiation stability are difficult, but qualitatively, our results strongly suggest the latter is much more stable to proton fluences than the other three polymorphs. We observed deep donor formation at E_C-0.65 eV upon hydrogenation of γ-Ga_2O_3, attributed to Si-H complexes, in the context of literature and assuming similarities with the behavior observed in β-Ga_2O_3. The evolution of the deep trap signatures in these samples upon irradiation featured the suppression of the E_C-0.65 eV trap and emergence of the E_C-0.3 eV and E_C-1 eV levels, both of which remain to be identified.

By contrast, without intentional introduction of silicon into γ-Ga_2O_3, upon hydrogenation we measured high electron concentrations, tentatively ascribed to the creation of V_{Ga}-4H complexes. The present work paves the way for further detailed studies of the double polymorph γ/β-Ga_2O_3 diodes, motivated both by interesting fundamental science and potential applications of such diodes in radiation harsh environments.

Author Contributions

Conceptualization, A.Y.P., A.K. and S.J.P.; data curation, A.Y.P., A.A.V., A.I.K., A.K. and S.J.P; formal analysis, A.Y.P., E.B.Y., A.K., A.A. and S.J.P.; funding acquisition, A.Y.P., E.B.Y., A.K. and S.J.P.; investigation, A.Y.P., A.A.V., I.V.S, A.I.K., E.B.Y., A.A.R., L.A.A., and N.M.; methodology, A.Y.P., A.A.V., I.V.S, A.I.K., E.B.Y., A.V.C., L.P.B., A.S.D., R.Sh.I., A.A.; project administration, A.Y.P., E.B.Y., A.K. and S.J.P.; resources, A.K., A.A., A.V.M., A.V.C., P.B.L., Y.S.P., A.S.D. and R.Sh.I.; software, A.Y.P., A.A.V., I.V.S., S.J.P.; supervision, A.Y.P., A.K. and S.J.P.; validation, A.Y.P., E.B.Y., A.K. and S.J.P.; visualization, A.Y.P., S.J.P., A.A.V. and A.I.K.; writing—original draft, A.Y.P., A.K. and S.J.P.; writing—review and editing, A.A.V., A.I.K. and I.V.S.; visualization, A.Y.P., S.J.P., A.A.V. and A.I.K.; supervision, S.J.P.; project administration, A.Y.P.; funding acquisition, E.B.Y., A.K. and S.J.P. All authors have read and agreed to the published version of the manuscript

Conflicts of interest

There are no conflicts to declare.

Acknowledgements

The work at NUST MISIS was supported in part by a grant from the Ministry of Science and Higher Education of Russian Federation (Agreement # 075-15-2022-1113). The work at the University of Oslo was enabled by the M-ERA.NET funds administrated by the Research Council of Norway via project number 337627 as well as the INTPART program at the Research Council of Norway via project No. 322382. The work at UF was performed as part of Interaction of Ionizing Radiation with Matter University Research Alliance (IIRM-URA), sponsored by the Department of the Defense, Defense Threat Reduction Agency under award HDTRA1–20–2–0002. The content of the information does not necessarily reflect the position or the policy of the federal government, and no official endorsement should be inferred. The data that supports the findings of this study are available within the article and its supplementary material.

References

1 S. J. Pearton, F. Ren, M. Tadjer and J. Kim, *J Appl Phys*, 2018, **124**, DOI:10.1063/1.5062841.
2 Masataka Higashiwaki and Shizuo Fujita, Eds., *Gallium Oxide: Materials Properties, Crystal Growth, and Devices*, Springer International Publishing, Cham, 2020.
3 J. Xu, W. Zheng and F. Huang, *J Mater Chem C Mater*, 2019, **7**, 8753–8770.
4 J. S. Speck and E. Farzana, Eds., *Ultrawide Bandgap β-Ga2O3 Semiconductor*, AIP Publishing, 2023.

5 K. Kaneko, S. Fujita and T. Hitora, *Jpn J Appl Phys*, 2018, **57**, 02CB18.
6 E. Ahmadi and Y. Oshima, *J Appl Phys*, 2019, **126**, DOI:10.1063/1.5123213.
7 J. Bae, J.-H. Park, D.-W. Jeon and J. Kim, *APL Mater*, 2021, **9**, DOI:10.1063/5.0067133.
8 A. Parisini, A. Bosio, V. Montedoro, A. Gorreri, A. Lamperti, M. Bosi, G. Garulli, S. Vantaggio and R. Fornari, *APL Mater*, 2019, **7**, DOI:10.1063/1.5050982.
9 A. Y. Polyakov, V. I. Nikolaev, E. B. Yakimov, F. Ren, S. J. Pearton and J. Kim, *Journal of Vacuum Science & Technology A*, 2022, **40**, DOI:10.1116/6.0001701.
10 E. B. Yakimov, A. Y. Polyakov, V. I. Nikolaev, A. I. Pechnikov, M. P. Scheglov, E. E. Yakimov and S. J. Pearton, *Nanomaterials*, 2023, **13**, 1214.
11 A. Azarov, J.-H. Park, D.-W. Jeon and A. Kuznetsov, *Appl Phys Lett*, 2023, **122**, DOI:10.1063/5.0149870.
12 E. A. Anber, D. Foley, A. C. Lang, J. Nathaniel, J. L. Hart, M. J. Tadjer, K. D. Hobart, S. Pearton and M. L. Taheri, *Appl Phys Lett*, 2020, **117**, DOI:10.1063/5.0022170.
13 A. Azarov, C. Bazioti, V. Venkatachalapathy, P. Vajeeston, E. Monakhov and A. Kuznetsov, *Phys Rev Lett*, 2022, **128**, 015704.
14 H.-L. Huang, C. Chae, J. M. Johnson, A. Senckowski, S. Sharma, U. Singisetti, M. H. Wong and J. Hwang, *APL Mater*, 2023, **11**, DOI:10.1063/5.0134467.
15 A. Azarov, J. G. Fernández, J. Zhao, F. Djurabekova, H. He, R. He, Ø. Prytz, L. Vines, U. Bektas, P. Chekhonin, N. Klingner, G. Hlawacek and A. Kuznetsov, *Nat Commun*, 2023, **14**, 4855.
16 Javier García Fernández submitted, *Adv Mater Interfaces*.
17 A. Y. Polyakov, A. I. Kochkova, A. Azarov, V. Venkatachalapathy, A. V. Miakonkikh, A. A. Vasilev, A. V. Chernykh, I. V. Shchemerov, A. A. Romanov, A. Kuznetsov and S. J. Pearton, *J Appl Phys*, 2023, **133**, DOI:10.1063/5.0133181.
18 R. Sharma, M. E. Law, F. Ren, A. Y. Polyakov and S. J. Pearton, *Journal of Vacuum Science & Technology A: Vacuum, Surfaces, and Films*, , DOI:10.1116/6.0001307.
19 J. B. Varley, H. Peelaers, A. Janotti and C. G. Van de Walle, *Journal of Physics: Condensed Matter*, 2011, **23**, 334212.
20 A. Y. Polyakov, E. B. Yakimov, V. I. Nikolaev, A. I. Pechnikov, A. V. Miakonkikh, A. Azarov, I.-H. Lee, A. A. Vasilev, A. I. Kochkova, I. V. Shchemerov, A. Kuznetsov and S. J. Pearton, *Crystals (Basel)*, 2023, **13**, 1400.
21 E. B. Yakimov, A. Y. Polyakov, I. V. Shchemerov, N. B. Smirnov, A. A. Vasilev, A. I. Kochkova, P. S. Vergeles, E. E. Yakimov, A. V. Chernykh, M. Xian, F. Ren and S. J. Pearton, *J Alloys Compd*, 2021, **879**, 160394.
22 H. He, C. Wu, H. Hu, S. Wang, F. Zhang, D. Guo and F. Wu, *J Phys Chem Lett*, 2023, **14**, 6444–6450.
23 J. Kim, S. J. Pearton, C. Fares, J. Yang, F. Ren, S. Kim and A. Y. Polyakov, *J Mater Chem C Mater*, 2019, **7**, 10–24.
24 S. J. Pearton, F. Ren, J. Kim, M. Stavola and A. Y. Polyakov, in *Wide Bandgap Semiconductor-Based Electronics*, IOP Publishing, 2020, pp. 7-1-7–21.
25 M. M. Chang, D. Y. Guo, X. L. Zhong, F. B. Zhang and J. B. Wang, *J Appl Phys*, 2022, **132**, DOI:10.1063/5.0105752.
26 A. Y. Polyakov, I. V. Shchemerov, A. A. Vasilev, A. I. Kochkova, N. B. Smirnov, A. V. Chernykh, E. B. Yakimov, P. B. Lagov, Yu. S. Pavlov, E. M. Ivanov, O. G. Gorbatkova, A. S. Drenin, M. E. Letovaltseva, M. Xian, F. Ren, J. Kim and S. J. Pearton, *J Appl Phys*, 2021, **130**, DOI:10.1063/5.0068306.
27 S. J. Pearton, A. Aitkaliyeva, M. Xian, F. Ren, A. Khachatrian, A. Ildefonso, Z. Islam, M. A. Jafar Rasel, A. Haque, A. Y. Polyakov and J. Kim, *ECS Journal of Solid State Science and Technology*, 2021, **10**, 055008.
28 W.-S. Ai, J. Liu, Q. Feng, P.-F. Zhai, P.-P. Hu, J. Zeng, S.-X. Zhang, Z.-Z. Li, L. Liu, X.-Y. Yan and Y.-M. Sun, *Chinese Physics B*, 2021, **30**, 056110.
29 A. Y. Polyakov, A. Kuznetsov, A. Azarov, A. V. Miakonkikh, A. V. Chernykh, A. A. Vasilev, I. V. Shchemerov, A. I. Kochkova, N. R. Matros and S. J. Pearton, *Journal of Materials Science: Materials in Electronics*, 2023, **34**, 1201.
30 M. E. Ingebrigtsen, A. Yu. Kuznetsov, B. G. Svensson, G. Alfieri, A. Mihaila, U. Badstübner, A. Perron, L. Vines and J. B. Varley, *APL Mater*, 2019, **7**, DOI:10.1063/1.5054826.
31 A. Azarov, V. Venkatachalapathy, I.-H. Lee and A. Kuznetsov, *Journal of Vacuum Science & Technology A*, 2023, **41**, DOI:10.1116/6.0002388.
32 Z. Zhang, E. Farzana, A. R. Arehart and S. A. Ringel, *Appl Phys Lett*, 2016, **108**, DOI:10.1063/1.4941429.
33 A. Y. Polyakov, N. B. Smirnov, I.-H. Lee and S. J. Pearton, *Journal of Vacuum Science & Technology B, Nanotechnology and Microelectronics: Materials, Processing, Measurement, and Phenomena*, 2015, **33**, DOI:10.1116/1.4932013.
34 A. Y. Polyakov, V. I. Nikolaev, A. I. Pechnikov, P. B. Lagov, I. V Shchemerov, A. A. Vasilev, A. V Chernykh, A. I. Kochkova, L. Guzilova, Y. S. Pavlov, T. V Kulevoy, A. S. Doroshkevich, R. S. Isaev, A. V Panichkin and S. J. Pearton, *J Phys D Appl Phys*, 2023, **56**, 305103.
35 A. Y. Polyakov, N. B. Smirnov, I. V. Shchemerov, S. J. Pearton, F. Ren, A. V. Chernykh and A. I. Kochkova, *Appl Phys Lett*, 2018, **113**, DOI:10.1063/1.5051986.
36 A. Y. Polyakov, N. B. Smirnov, I. V. Shchemerov, S. J. Pearton, F. Ren, A. V. Chernykh, P. B. Lagov and T. V. Kulevoy, *APL Mater*, 2018, **6**, DOI:10.1063/1.5042646.
37 A. Y. Polyakov, N. M. Shmidt, N. B. Smirnov, I. V. Shchemerov, E. I. Shabunina, N. A. Tal'nishnih, I.-H. Lee, L. A. Alexanyan, S. A. Tarelkin and S. J. Pearton, *J Appl Phys*, 2019, **125**, DOI:10.1063/1.5093723.
38 A. Y. Polyakov, A. I. Kochkova, A. Langørgen, L. Vines, A. Vasilev, I. V. Shchemerov, A. A. Romanov and S. J. Pearton, *Journal of Vacuum Science & Technology A*, 2023, **41**, DOI:10.1116/6.0002307.
39 A. Langørgen, C. Zimmermann, Y. Kalmann Frodason, E. Førdestrøm Verhoeven, P. Michael Weiser, R. Michael Karsthof, J. Basile Varley and L. Vines, *J Appl Phys*, 2022, **131**, DOI:10.1063/5.0083861.
40 A. Y. Polyakov, I.-H. Lee, A. Miakonkikh, A. V. Chernykh, N. B. Smirnov, I. V. Shchemerov, A. I. Kochkova, A. A. Vasilev and S. J. Pearton, *J Appl Phys*, 2020, **127**, DOI:10.1063/1.5145277.
41 A. Polyakov, I. Lee, V. Nikolaev, A. Pechnikov, A. Miakonkikh, M. Scheglov, E. Yakimov, A. Chikiryaka, A. Vasilev, A. Kochkova, I. Shchemerov, A. Chernykh and S. Pearton, *Adv Mater Interfaces*, 2023, DOI:10.1002/admi.202300394.
42 M. M. Islam, M. O. Liedke, D. Winarski, M. Butterling, A. Wagner, P. Hosemann, Y. Wang, B. Uberuaga and F. A. Selim, *Sci Rep*, 2020, **10**, 6134.
43 A. Venzie, A. Portoff, M. Stavola, W. B. Fowler, J. Kim, D.-W. Jeon, J.-H. Park and S. J. Pearton, *Appl Phys Lett*, 2022, **120**, DOI:10.1063/5.0094707.
44 T. Kobayashi, T. Gake, Y. Kumagai, F. Oba and Y. Matsushita, *Applied Physics Express*, 2019, **12**, 091001.